




Cite this: *Nanoscale*, 2024, **16**, 11090

[Au₉Ag₆(C≡CR)₁₀(DPPM)₂Cl₂](PPh₄): a four-electron cluster with a bi-decahedral twisted metal core†

Guocheng Deng,^{‡a,b} Taeyoung Ki,^{‡a,b} Seungwoo Yoo,^{a,b} Xiaolin Liu,^{a,b} Kangjae Lee,^{a,b} Megalamane S. Bootharaju^{*a,b} and Taeghwan Hyeon ^{*a,b}

The assembly of cluster units in a distinct manner can give rise to nanoclusters exhibiting unique geometrical structures and properties. Herein, we present a one-pot synthesis and structural characterization of a AuAg alloy cluster, [Au₉Ag₆(C≡CR)₁₀(DPPM)₂Cl₂](PPh₄), denoted as **Au₉Ag₆** (where HC≡CR is 3,5-bis(trifluoromethyl)phenylacetylene, and DPPM is bis(diphenylphosphino)methane). Single-crystal X-ray diffraction data analysis reveals that **Au₉Ag₆** features a distinctive Au₇Ag₆ bi-decahedral core, formed by a twisted assembly of two Au₄Ag₃ decahedra sharing one vertex. The Au₄Ag₃ building blocks are bridged by two gold atoms on opposite sides of the bi-decahedral core. The **Au₉Ag₆** cluster is monoanionic and it is stabilized by two chloride, two DPPM and ten alkynyl ligands. This cluster represents the first instance of a cluster of clusters built upon decahedral units.

Received 4th April 2024,
Accepted 6th May 2024

DOI: 10.1039/d4nr01471e

rsc.li/nanoscale

Introduction

Significant efforts have been dedicated to synthesizing metal clusters with diverse structures in order to obtain clusters endowed with distinctive properties for a variety of potential applications.^{1–6} With the advancement of sophisticated characterization techniques, numerous metal clusters with atomic-level resolved structures have been reported to date.^{7–21} It has been observed that the metal core of many of these clusters shares the same polyhedral units, despite variations in peripheral ligands or metal–ligand motif structures. These polyhedral units encompass an M₁₃ centered icosahedron,^{22–28} an M₆ octahedron,^{29–35} an M₁₃ cuboctahedron³⁶ and an M₇ decahedron,^{37–42} among others, where ‘M’ represents Au, Ag, Cu, or other metal atoms or their mixtures. These fundamental polyhedral units can also be assembled through the sharing of vertices, edges, or faces, expanding the range of structural types for clusters. Such clusters are referred to as ‘cluster of clusters’.⁴³

The centered icosahedron serves as a classic assembly component. To date, many Au, Ag or their alloy clusters, featuring metal cores with rod-shaped bi-icosahedral,^{44–48} rod-shaped

tri-icosahedral,^{49,50} ring-shaped tri-icosahedral,⁴³ rod-shaped tetra-icosahedral,⁵¹ or ring-shaped penta-icosahedral structures,⁵² have been reported. The Wang group reported an Au cluster, [Au₂₄(C≡CPh)₁₄(PPh₃)₄](SbF₆)₂, which contains two cuboctahedral units by sharing of faces.³⁶ Additionally, the assembly of octahedral units by sharing vertices has been observed in Ag clusters such as Ag₂₃(PPh₃)₈(SC₂H₄Ph)₁₈,²⁹ [Ag₃₈(SPhF₂)₂₆(PR′₃)₈] and [Ag₆₃(SPhF₂)₃₆(PR′₃)₈]⁺ (HSPHF₂ = 3,4-difluorothiophenol and R′ = alkyl/aryl).³² Recently, Wang *et al.* reported the largest structurally characterized cluster of clusters to date, [Ag₉₃(PPh₃)₆(C≡CR)₅₀]³⁺ (R = 4-CH₃OC₆H₄).⁵³ This cluster features a Ag₆₉ core consisting of a bicapped hexagonal prismatic Ag₁₅ unit, which is wrapped by six Ino decahedra through sharing of edges. It is worth mentioning that the assembled entities from the same polyhedral units usually exhibit different physical and chemical properties, indicating the great potential of cluster of clusters families for applications.^{50,51}

A decahedron is commonly found as a polyhedral unit in clusters; however, the existence of cluster of clusters based on it has not been reported to date. In this study, we report an alkynyl-protected AuAg alloy cluster that features a bi-decahedral core, formed by two decahedra sharing one vertex. The molecular formula of the cluster is [Au₉Ag₆(C≡CR)₁₀(DPPM)₂Cl₂](PPh₄), denoted as **Au₉Ag₆** (where HC≡CR is 3,5-bis(trifluoromethyl)phenylacetylene; DPPM is bis(diphenylphosphino)methane). The definite composition, atomic-level structure and optical properties of **Au₉Ag₆** are thoroughly characterized by a range of analytical techniques, including electrospray ionization time of flight mass spectrometry (ESI-TOF-MS), elemental analysis, single-crystal X-ray diffraction (SCXRD), and optical spec-

^aCenter for Nanoparticle Research, Institute for Basic Science (IBS), Seoul 08826, Republic of Korea. E-mail: msbootharaju@snu.ac.kr, thyeon@snu.ac.kr

^bSchool of Chemical and Biological Engineering, and Institute of Chemical Processes, Seoul National University, Seoul 08826, Republic of Korea

†Electronic supplementary information (ESI) available: Experimental details, additional characterization table, and figures. CCDC 2343939. For ESI and crystallographic data in CIF or other electronic format see DOI: <https://doi.org/10.1039/d4nr01471e>

‡These authors contributed equally to this work.



troscopy. This structure reveals the assembly of decahedral structural units for the first time, thereby broadening the scope of cluster of clusters.

Experimental section

Reagents

Hydrogen tetrachloroaurate(III) trihydrate ($\text{HAuCl}_4 \cdot 3\text{H}_2\text{O}$) was purchased from Strem. Triethylamine (Et_3N), silver nitrate (AgNO_3), bis(diphenylphosphino)methane (DPPM), and tetraphenylphosphonium chloride (PPh_4Cl) were purchased from Sigma-Aldrich. 3,5-Bis(trifluoromethyl)phenylacetylene ($\text{HC}\equiv\text{CR}$), dimethyl sulfide ($(\text{CH}_3)_2\text{S}$) and sodium borohydride (NaBH_4) were purchased from TCI. Dichloromethane (CH_2Cl_2), methanol (CH_3OH), ethanol ($\text{C}_2\text{H}_5\text{OH}$), acetonitrile (CH_3CN), acetone ($\text{C}_3\text{H}_6\text{O}$), chloroform (CHCl_3), *N,N*-dimethylformamide (DMF), tetrahydrofuran (THF) and *n*-hexane (C_6H_{14}) were purchased from Samchun. AuSMe_2Cl was prepared according to a literature method.⁸ All reagents were used as received without further purification. The water used in all experiments was ultrapure.

Synthesis of $\text{AgC}\equiv\text{CR}$

510 mg of AgNO_3 was dissolved in 35 mL of acetonitrile, followed by the addition of 531 μL of 3,5-bis(trifluoromethyl)phenylacetylene. Subsequently, 500 μL of triethylamine was added to the solution with vigorous stirring. The reaction mixture was stirred for 4 hours at room temperature in the absence of light. The obtained turbid mixture was centrifuged at 6000 rpm for 5 min. The precipitate was washed with 50 mL of methanol and then dried under vacuum at room temperature to obtain a gray $\text{AgC}\equiv\text{CR}$ complex. The yield of $\text{AgC}\equiv\text{CR}$ was ~78% (based on Ag).

Synthesis of the Au_9Ag_6 cluster

11.8 mg of AuSMe_2Cl was dissolved in 4 mL of CH_2Cl_2 . Subsequently, a solution of 7.7 mg of DPPM in 2 mL of CH_2Cl_2 was added to the above solution under vigorous stirring (500 rpm). After magnetically stirring the solution for 5 minutes, 13.8 mg of $\text{AgC}\equiv\text{CR}$ solid was added. Following that, a solution of 2 mg of PPh_4Cl in 1 mL of CH_2Cl_2 , and 6 μL of triethylamine were sequentially added. After 5 minutes, a solution of NaBH_4 (0.2 mg in 1 mL of ethanol) was added dropwise. The solution was left to age for 24 hours. The resulting solution was washed with water. The aqueous phase was removed, and the organic phase was centrifuged at 12 000 rpm for 3 minutes. The precipitate was discarded, and the organic solution was subjected to diffusion of *n*-hexane at room temperature. After 7 days, dark-brown block crystals were obtained with a yield of 16% (based on Au).

Physical measurements

The UV/vis/NIR absorption spectra were recorded using a Cary 5000 spectrophotometer (Agilent). The scanning electron microscopy energy dispersive X-ray spectroscopy (SEM-EDS)

analysis was performed on a JSM-7800F Prime microscope (JEOL, Japan). The electrospray ionization mass spectrometry (ESI-MS) analysis was performed using an ESI-TOF mass spectrometer (6224, Agilent, Santa Clara, CA, USA).

Single crystal structure analysis

The diffraction data of Au_9Ag_6 were collected using an X-ray single crystal diffractometer with Cu $K\alpha$ radiation ($\lambda = 1.54184 \text{ \AA}$) at 100 K on a Rigaku XtaLab Synergy R system. The data were processed using CrysAlis^{Pro}. The structure was solved and refined using full-matrix least-squares based on F^2 with ShelXT and ShelXL programs within Olex2. More refined data are provided in Table S1.†

Results and discussion

The Au_9Ag_6 cluster was synthesized *via* a one-pot method at room temperature (Scheme 1). Specifically, a gold precursor (Me_2SAuCl), a diphosphine ligand (DPPM), a silver precursor ($\text{AgC}\equiv\text{CR}$), and a counter cation (PPh_4^+) were sequentially added to a dichloromethane (CH_2Cl_2) solution. Subsequently, an ethanol solution of sodium borohydride (NaBH_4) was introduced (see the Experimental section for more synthetic details). After 24 hours of reaction, the organic layer was washed with water. Then, *n*-hexane was introduced into the organic layer of the crude products. Dark-brown block-like single crystals (Fig. S1†) were obtained after a week.

The composition of the Au_9Ag_6 cluster was unambiguously determined by ESI-TOF-MS in the negative-ion mode. As shown in Fig. 1, only a single peak at $m/z = 5630.42$ was observed, precisely corresponding to the molecular ion $[\text{Au}_9\text{Ag}_6(\text{C}\equiv\text{CR})_{10}(\text{DPPM})_2\text{Cl}_2]^-$ (calculated $m/z = 5630.44$). The experimental isotopic pattern of the monoanionic cluster exhibited remarkable concordance with the simulated pattern (Fig. 1, inset). These ESI-TOF-MS results conclusively establish that the Au_9Ag_6 cluster possesses a -1 charge and excludes any positional disorder among the Au and Ag atoms within the cluster. Furthermore, the scanning electron microscopy energy dispersive X-ray spectroscopy (SEM EDS) analysis confirmed the presence of Au, Ag, P, Cl, and F elements in the Au_9Ag_6 cluster (Fig. S2 and S3†).

The atomically precise structure of the Au_9Ag_6 cluster was determined using SCXRD, revealing that it adopts a triclinic crystal system with the space group $P\bar{1}$ (no. 2) (Table S1 and Fig. S4†). The packing diagram of Au_9Ag_6 illustrates the presence of two independent clusters in the unit cell (Fig. S5†). Additionally, two counter cations (PPh_4^+) were observed in the unit cell (Fig. S5†), further confirming the -1 charge of the



Scheme 1 Synthetic route to the Au_9Ag_6 cluster.



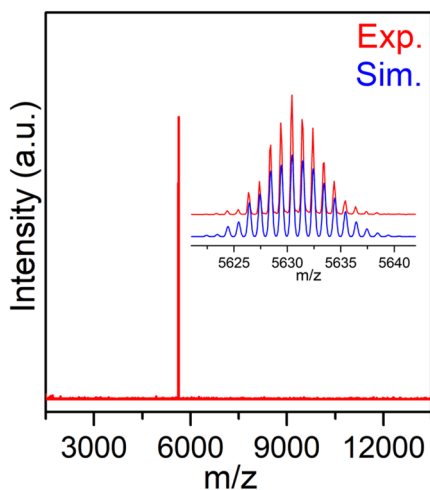


Fig. 1 Mass spectrum of the Au_9Ag_6 cluster in the negative-ion mode. Inset: the measured (red trace) and simulated (blue trace) isotopic patterns of $[\text{Au}_9\text{Ag}_6(\text{C}\equiv\text{CR})_{10}(\text{DPPM})_2\text{Cl}_2]^-$.

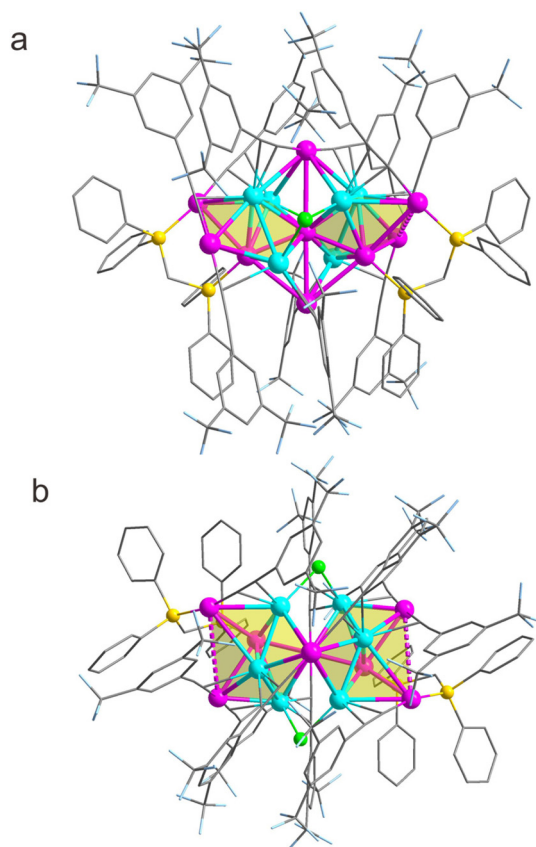


Fig. 2 Overall structure of the Au_9Ag_6 cluster. (a) Side view. (b) Top view. Color legend: magenta, Au; turquoise, Ag; yellow, P; green, Cl; pale blue, F; and gray, C. All hydrogen atoms are omitted for clarity.

cluster, which is strongly supported by the ESI-TOF-MS data (Fig. 1). The side- and top-views of the Au_9Ag_6 cluster are shown in Fig. 2a and b, respectively, demonstrating that the cluster comprises nine gold atoms, six silver atoms, 10 $\text{C}\equiv\text{CR}$

ligands, two DPPM ligands and two chlorides, resulting in the molecular formula $\text{Au}_9\text{Ag}_6(\text{C}\equiv\text{CR})_{10}(\text{DPPM})_2\text{Cl}_2$. This composition is consistent with that obtained by mass spectrometry (Fig. 1). According to the “superatom electronic theory”,⁵⁴ the free metallic electron count of this cluster is calculated to be four ($9 + 6 - 10 - 2 + 1 = 4$), indicating that the cluster has an open-shell electronic structure.

A detailed analysis of the molecular architecture of the Au_9Ag_6 cluster revealed that it possesses a bi-decahedral core. As shown in Fig. 3a, this cluster contains two Au_4Ag_3 decahedra, where one silver atom and one gold atom occupy the top and bottom of each decahedron, respectively. Their pentagonal planes consist of two silver and three gold atoms (Fig. 3a). In comparison with the ideal decahedron, both Au_4Ag_3 decahedra in Au_9Ag_6 exhibit distortion (Fig. S6†). These two distorted Au_4Ag_3 decahedra assemble to form the Au_7Ag_6 bi-decahedral core by sharing a gold atom (Fig. 3b). Interestingly, upon assembly of these two decahedra, one of them rotates by 60.5° along the pentagonal plane (Fig. 3b). These factors result in the Au_7Ag_6 bi-decahedral core having C_2 symmetry, thus rendering it chiral (Fig. S7a†). This chirality extends from the

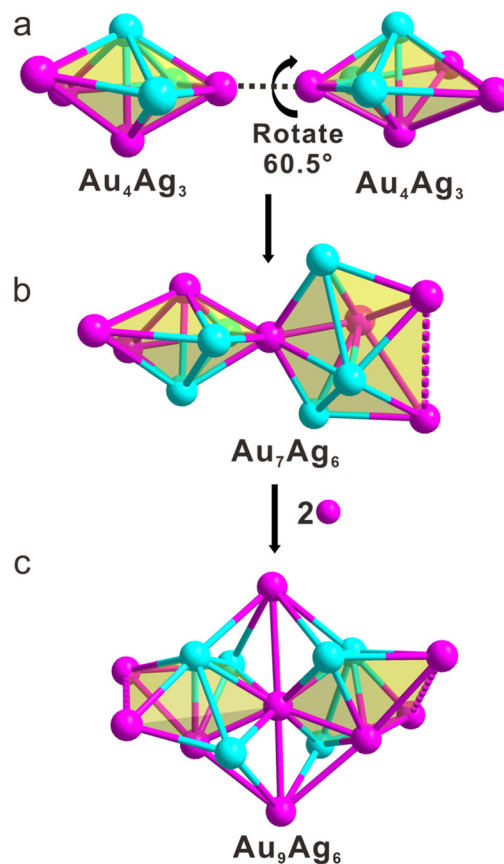


Fig. 3 Structural analysis of the Au_9Ag_6 cluster. (a) Structure of the distorted Au_4Ag_3 decahedron. (b) Two Au_4Ag_3 decahedra assemble into the Au_7Ag_6 bi-decahedral core. (c) Two gold atoms bridge the bi-decahedral core, forming the structure of Au_9Ag_6 . Color legend: magenta, Au and turquoise, Ag.



Au_7Ag_6 bi-decahedral core to the entire cluster, thereby imparting C_2 symmetry and chirality to the Au_9Ag_6 cluster (Fig. S7b†).

As shown in Fig. 3c, the Au_7Ag_6 bi-decahedral core is further linked by two gold atoms, forming the metal part, Au_9Ag_6 , of the cluster. These two gold atoms are positioned at the top and bottom of the cluster (Fig. 2 and 3c). Both of these gold atoms coordinate with the gold atom shared by the two Au_4Ag_3 icosahedra and are situated on the C_2 axis (Fig. 2 and 3c). Additionally, the gold atom at the top coordinates with the four silver atoms of the bi-decahedron, while the gold atom at the bottom coordinates with the two silver atoms and two gold atoms of the bi-decahedron, thereby connecting the two decahedra (Fig. 3c). The average Ag–Ag and Au–Au distances in the cluster are 3.036 and 3.084 Å, respectively. Both of these distances are much longer than the Ag–Ag (2.889 Å) or Au–Au (2.884 Å) bond lengths found in bulk face-centered-cubic Ag or Au. The Au–Ag bond lengths in the cluster range from 2.702 to 3.438 Å, with an average of 2.975 Å.

The coordination modes of the surface ligands on the Au_9Ag_6 cluster were then analyzed. As shown in Fig. 2, the two chloride ligands, similar to the two gold atoms at the top and bottom of the cluster, serve to bridge the two Au_4Ag_3 decahedra. The distinction lies in the orientation of these two chlorine atoms, which are perpendicular to the C_2 axis and are disubstituted preferentially with silver atoms from different decahedra (Fig. 2). However, the two DPPM ligands are respectively coordinated to the two Au_4Ag_3 decahedra. They share the same coordination environment, coordinating preferentially with the gold atom at the bottom of the Au_4Ag_3 decahedron and one gold atom of the pentagonal planes through phosphorus atoms (Fig. 2). Interestingly, all ten alkynyl ligands on the Au_9Ag_6 cluster surface coordinate with gold through the σ bond and with silver through the π bond (Fig. 2). As shown in Fig. S8,† the ten alkynyl ligands on the cluster exhibit only one coordination mode: coordination with one Au atom *via* a σ bond and one Ag atom *via* a π bond in μ_2 mode. Such a simple coordination mode of alkynyl ligands on a cluster surface is very rare as compared to the complex binding modes of other clusters.^{25,55,56} The average Ag–Cl and Au–P bond lengths in the Au_9Ag_6 cluster are 2.536 and 2.293 Å, respectively. The Au–C and Ag–C bond lengths fall within the range of 1.969–2.058 and 2.351–2.569 Å, respectively.

The optical properties of the Au_9Ag_6 cluster were examined through UV/vis/NIR absorption spectroscopy. The UV/vis/NIR spectrum of the crystals of this cluster in CH_2Cl_2 solution is shown in Fig. 4. It reveals a prominent peak at 429 nm, accompanied by a shoulder peak at 384 nm, and two minor peaks at 538 and 620 nm. The crystals of Au_9Ag_6 are soluble in a wide range of commonly used organic solvents, including methanol, acetone, and acetonitrile (Fig. S9†). This solubility in various solvents is attributed to the presence of abundant F in the ligands of the cluster surface. Upon comparing the UV/vis spectrum of the cluster crystals with that of the as-prepared crude product, similar absorption peaks are observed (Fig. S10†), suggesting a good yield of the clusters. The UV/vis spectrum of the crystals of Au_9Ag_6 remains unchanged even

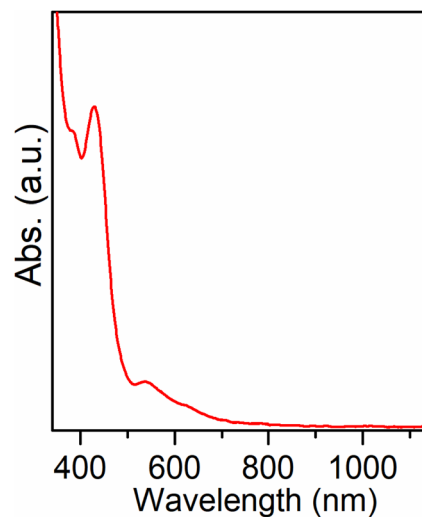


Fig. 4 UV/vis/NIR absorption spectrum of the Au_9Ag_6 cluster.

after exposure to air for one year (Fig. S11†), indicating its high ambient stability. As mentioned above, the Au_9Ag_6 cluster possesses an open-shell electronic structure. This characteristic resembles that of the highly stable rod-shaped $[\text{Au}_{25}(\text{PPh}_3)_{10}(\text{SC}_2\text{H}_5)_5\text{Cl}_2](\text{SbF}_6)_2$ (Au_{25}) cluster,⁴⁴ which comprises two Au_{13} icosahedra and exhibits an open-shell electronic structure with 16 (8 + 8) free electrons. Au_9Ag_6 contains two Au_4Ag_3 decahedra and has 4 (2 + 2) free electrons, which could be a contributing factor to the good stability of the clusters.

Conclusions

In summary, we have successfully synthesized and characterized a bimetallic AuAg cluster, $[\text{Au}_9\text{Ag}_6(\text{C}\equiv\text{CR})_{10}(\text{DPPM})_2\text{Cl}_2](\text{PPh}_4)$. Single crystal structure data analysis reveals that the core of this cluster adopts an Au_7Ag_6 bi-decahedral structure, formed by the twisted assembly of two Au_4Ag_3 decahedra sharing one gold vertex. This Au_7Ag_6 bi-decahedron core is further linked by two gold atoms and two chlorine atoms, and protected by two DPPM ligands and ten alkynyl ligands. Notably, this cluster represents the first example of a decahedron-based cluster of clusters. This study not only expands the repertoire of cluster of clusters families but also introduces novel strategies for obtaining clusters with diverse structures and properties, paving the way for their application across various fields.

Author contributions

G. D., X. L. and M. S. B. wrote the manuscript. G. D. and T. K. prepared the cluster samples. G. D., S. Y. and K. L. conducted the characterization studies. T. H. supervised the project. All authors commented on and agreed on the manuscript.



Conflicts of interest

There are no conflicts to declare.

Acknowledgements

T. H. acknowledges the financial support by the Research Center Program of the IBS (IBS-R006-D1) in Korea. M. S. B. acknowledges the IBS for the Young Scientist Fellowship (IBS-R006-Y2).

References

- I. Chakraborty and T. Pradeep, *Chem. Rev.*, 2017, **117**, 8208–8271.
- R. Jin, C. Zeng, M. Zhou and Y. Chen, *Chem. Rev.*, 2016, **116**, 10346–10413.
- Q. Yao, X. Yuan, T. Chen, D. Leong and J. Xie, *Adv. Mater.*, 2018, **30**, 1802751.
- D. Yang, Y. Sun, X. Cai, W. Hu, Y. Dai, Y. Zhu and Y. Yang, *CCS Chem.*, 2022, **4**, 66–94.
- J. Sun, X. Tang, Z. H. Liu, Z. Xie, B. Yan, C. Chaolumen, J. Zhang, W. Fang, W. Fang and H. Shen, *ACS Mater. Lett.*, 2024, **6**, 281–289.
- T. Chen, Q. Yao, R. R. Nasaruddin and J. Xie, *Angew. Chem., Int. Ed.*, 2019, **58**, 11967–11977.
- H. N. Qin, M. W. He, J. Wang, H. Y. Li, Z. Y. Wang, S. Q. Zang and T. C. W. Mak, *J. Am. Chem. Soc.*, 2024, **146**, 3545–3552.
- G. Deng, H. Yun, M. S. Bootharaju, F. Sun, K. Lee, X. Liu, S. Yoo, Q. Tang, Y. J. Hwang and T. Hyeon, *J. Am. Chem. Soc.*, 2023, **145**, 27407–27414.
- X. Wang, B. Yin, L. Jiang, C. Yang, Y. Liu, G. Zou, S. Chen and M. Zhu, *Science*, 2023, **381**, 784–790.
- P. Yuan, H. Zhang, Y. Zhou, T. Y. He, S. Malola, L. Gutierrez-Arzaluz, Y. Li, G. Deng, C. Dong, R. Huang, X. Song, B. K. Teo, O. F. Mohammed, H. Häkkinen, O. M. Bakr and N. Zheng, *Aggregate*, 2024, **5**, e475.
- W.-Q. Shi, L. Zeng, R.-L. He, X.-S. Han, Z.-J. Guan, M. Zhou and Q.-M. Wang, *Science*, 2024, **383**, 326–330.
- B. Yan, X. You, X. Tang, J. Sun, Q. Xu, L. Wang, Z.-J. Guan, F. Li and H. Shen, *Chem. Mater.*, 2024, **36**, 1004–1012.
- Y.-L. Gao, X. Sun, X. Tang, Z. Xie, G. Tian, Z.-A. Nan, H. Yang and H. Shen, *Dalton Trans.*, 2023, **52**, 52–57.
- T. Jia, Z. J. Guan, C. Zhang, X. Z. Zhu, Y. X. Chen, Q. Zhang, Y. Yang and D. Sun, *J. Am. Chem. Soc.*, 2023, **145**, 10355–10363.
- G. Deng, J. Kim, M. S. Bootharaju, F. Sun, K. Lee, Q. Tang, Y. J. Hwang and T. Hyeon, *J. Am. Chem. Soc.*, 2023, **145**, 3401–3407.
- S. Wang, W. He, Y. Cui, Z. Zhou, L. Ma and S.-Q. Zang, *Nanoscale*, 2023, **15**, 12679–12685.
- A. K. Das, S. Biswas, A. Pal, S. S. Manna, A. Sardar, P. K. Mondal, B. Sahoo, B. Pathak and S. Mandal, *Nanoscale*, 2024, **16**, 3583–3590.
- Y. Liu, Z. Li, X.-H. Liu, N. Pinna and Y. Wang, *Nanoscale Horiz.*, 2023, **8**, 1435–1439.
- Z. Xu, H. Dong, W. Gu, Z. He, F. Jin, C. Wang, Q. You, J. Li, H. Deng, L. Liao, D. Chen, J. Yang and Z. Wu, *Angew. Chem., Int. Ed.*, 2023, **62**, e202308441.
- S. Zhuang, D. Chen, Q. You, W. Fan, J. Yang and Z. Wu, *Angew. Chem., Int. Ed.*, 2022, **61**, e202208751.
- M. Wang, S. Li, X. Tang, D. Zuo, Y. Jia, S. Guo, Z.-J. Guan and H. Shen, *Phys. Chem. Chem. Phys.*, 2023, **25**, 30373–30380.
- E. L. Albright, S. Malola, S. I. Jacob, H. Yi, S. Takano, K. Mimura, T. Tsukuda, H. Häkkinen, M. Nambo and C. M. Crudden, *Chem. Mater.*, 2024, **36**, 1279–1289.
- J. Q. Fan, Y. Yang, C. B. Tao and M. B. Li, *Angew. Chem., Int. Ed.*, 2023, **62**, e202215741.
- M. Zhou, K. Li, P. Wang, H. Zhou, S. Jin, Y. Pei and M. Zhu, *Nanoscale*, 2023, **15**, 2633–2641.
- G. Deng, K. Lee, H. Deng, S. Malola, M. S. Bootharaju, H. Häkkinen, N. Zheng and T. Hyeon, *Angew. Chem., Int. Ed.*, 2023, **62**, e202217483.
- S. Jin, X. Zou, L. Xiong, W. Du, S. Wang, Y. Pei and M. Zhu, *Angew. Chem., Int. Ed.*, 2018, **57**, 16768–16772.
- S. F. Yuan, Z. J. Guan and Q. M. Wang, *J. Am. Chem. Soc.*, 2022, **144**, 11405–11412.
- G. Deng, S. Malola, J. Yan, Y. Han, P. Yuan, C. Zhao, X. Yuan, S. Lin, Z. Tang, B. K. Teo, H. Häkkinen and N. Zheng, *Angew. Chem., Int. Ed.*, 2018, **57**, 3421–3425.
- C. Liu, T. Li, H. Abroshan, Z. Li, C. Zhang, H. J. Kim, G. Li and R. Jin, *Nat. Commun.*, 2018, **9**, 744.
- W.-D. Si, C. Zhang, M. Zhou, W.-D. Tian, Z. Wang, Q. Hu, K.-P. Song, L. Feng, X.-Q. Huang, Z.-Y. Gao, C.-H. Tung and D. Sun, *Sci. Adv.*, 2023, **9**, eadg3587.
- G. Deng, K. Lee, H. Deng, M. S. Bootharaju, N. Zheng and T. Hyeon, *J. Phys. Chem. C*, 2022, **126**, 20577–20583.
- H. Yang, J. Yan, Y. Wang, H. Su, L. Gell, X. Zhao, C. Xu, B. K. Teo, H. Häkkinen and N. Zheng, *J. Am. Chem. Soc.*, 2017, **139**, 31–34.
- A. Jose, A. Jana, T. Gupte, A. S. Nair, K. Unni, A. Nagar, A. R. Kini, B. K. Spoorthi, S. K. Jana, B. Pathak and T. Pradeep, *ACS Mater. Lett.*, 2023, **5**, 893–899.
- Z. Lei, M. Endo, H. Ube, T. Shiraogawa, P. Zhao, K. Nagata, X.-L. Pei, T. Eguchi, T. Kamachi, M. Ehara, T. Ozawa and M. Shionoya, *Nat. Commun.*, 2022, **13**, 4288.
- J. P. Dong, Y. Xu, X. G. Zhang, H. Zhang, L. Yao, R. Wang and S. Q. Zang, *Angew. Chem., Int. Ed.*, 2023, **62**, e202313648.
- X. K. Wan, W. W. Xu, S. F. Yuan, Y. Gao, X. C. Zeng and Q. M. Wang, *Angew. Chem., Int. Ed.*, 2015, **54**, 9683–9686.
- T. Higaki, C. Liu, M. Zhou, T. Y. Luo, N. L. Rosi and R. Jin, *J. Am. Chem. Soc.*, 2017, **139**, 9994–10001.
- Y. Song, Y. Li, H. Li, F. Ke, J. Xiang, C. Zhou, P. Li, M. Zhu and R. Jin, *Nat. Commun.*, 2020, **11**, 478.
- J. Yan, J. Zhang, X. Chen, S. Malola, B. Zhou, E. Selenius, X. Zhang, P. Yuan, G. Deng, K. Liu, H. Su, B. K. Teo, H. Häkkinen, L. Zheng and N. Zheng, *Natl. Sci. Rev.*, 2018, **5**, 694–702.



- 40 C.-G. Shi, J.-H. Jia, Y. Jia, G. Li and M.-L. Tong, *CCS Chem.*, 2023, **5**, 1154–1162.
- 41 X. Ma, S. He, Q. Li, Q. Li, J. Chai, W. Ma, G. Li, H. Yu and M. Zhu, *Inorg. Chem.*, 2023, **62**, 15680–15687.
- 42 J.-J. Li, Z. Liu, Z.-J. Guan, X.-S. Han, W.-Q. Shi and Q.-M. Wang, *J. Am. Chem. Soc.*, 2022, **144**, 690–694.
- 43 B. K. Teo, H. Zhang and X. Shi, *J. Am. Chem. Soc.*, 1990, **112**, 8552–8562.
- 44 Y. Shichibu, Y. Negishi, T. Watanabe, N. K. Chaki, H. Kawaguchi and T. Tsukuda, *J. Phys. Chem. C*, 2007, **111**, 7845–7847.
- 45 H. Shen, G. Deng, S. Kaappa, T. Tan, Y. Han, S. Malola, S. Lin, B. K. Teo, H. Häkkinen and N. Zheng, *Angew. Chem., Int. Ed.*, 2019, **58**, 17731–17735.
- 46 B. K. Teo and K. Keating, *J. Am. Chem. Soc.*, 1984, **106**, 2224–2226.
- 47 M. S. Bootharaju, S. M. Kozlov, Z. Cao, M. Harb, N. Maity, A. Shkurenko, M. R. Parida, M. N. Hedhili, M. Eddaoudi, O. F. Mohammed, O. M. Bakr, L. Cavallo and J. M. Basset, *J. Am. Chem. Soc.*, 2017, **139**, 1053–1056.
- 48 A. Ma, J. Wang, J. Kong, Y. Ren, Y. Wang, X. Ma, M. Zhou and S. Wang, *Phys. Chem. Chem. Phys.*, 2023, **25**, 9772–9778.
- 49 T. H. Chiu, J. H. Liao, F. Gam, I. Chantrenne, S. Kahlal, J. Y. Saillard and C. W. Liu, *J. Am. Chem. Soc.*, 2019, **141**, 12957–12961.
- 50 R. Jin, C. Liu, S. Zhao, A. Das, H. Xing, C. Gayathri, Y. Xing, N. L. Rosi, R. R. Gil and R. Jin, *ACS Nano*, 2015, **9**, 8530–8536.
- 51 S.-F. Yuan, C.-Q. Xu, W.-D. Liu, J.-X. Zhang, J. Li and Q.-M. Wang, *J. Am. Chem. Soc.*, 2021, **143**, 12261–12267.
- 52 Y. Song, F. Fu, J. Zhang, J. Chai, X. Kang, P. Li, S. Li, H. Zhou and M. Zhu, *Angew. Chem., Int. Ed.*, 2015, **54**, 8430–8434.
- 53 F. Hu, R.-L. He, Z.-J. Guan, C.-Y. Liu and Q.-M. Wang, *Angew. Chem., Int. Ed.*, 2023, **62**, e202304134.
- 54 M. Walter, J. Akola, O. Lopez-Acevedo, P. D. Jadzinsky, G. Calero, C. J. Ackerson, R. L. Whetten, H. Grönbeck and H. Häkkinen, *Proc. Natl. Acad. Sci. U. S. A.*, 2008, **105**, 9157–9162.
- 55 X. Sun, X. Tang, Y.-L. Gao, Y. Zhao, Q. Wu, D. Cao and H. Shen, *Nanoscale*, 2023, **15**, 2316–2322.
- 56 L. Qin, F. Sun, Z. Gong, G. Ma, Y. Chen, Q. Tang, L. Qiao, R. Wang, Z.-Q. Liu and Z. Tang, *ACS Nano*, 2023, **17**, 12747–12758.

